# Steady optical beam propagating through turbulent environment

XINGWANG KANG,<sup>1,2,3</sup> XIUTING YANG,<sup>1,2</sup> JIAN MA,<sup>4</sup> YUHANG REN,<sup>4</sup> XINLI LIANG,<sup>1</sup> HUAHUA WANG,<sup>4</sup> YANG LIU,<sup>5</sup> ZHIZI MING,<sup>6</sup> HAORAN DU,<sup>4</sup> XINGLIN ZHONG,<sup>6</sup> ZHIGANG CHEN,<sup>7</sup> LU GAO,<sup>4</sup> AND ZE ZHANG<sup>1,5,6,\*</sup>

**Abstract:** A steady optical beam (SOB) propagating stably in a disorder medium is constructed by using a specially designed aspherical lens. Our theoretical and experimental results show that the generated SOB exhibits much better propagation features with small divergence and long Rayleigh length, as well as weak deformation through turbulent environment as compared with a conventional Gaussian beam. The beam parameter product of the SOB reaches 49.40% of the Gaussian beam by multiple measurements within a certain distance range. The SOB may find applications in optical communications and optical detection in turbulent transmission conditions.

© 2022 Optica Publishing Group under the terms of the Optica Open Access Publishing Agreement

#### 1. Introduction

Air turbulence is always a serious problem in applications that laser beam propagate through air or water medium, such as laser communication, Lidar or laser illumination [1–3]. Typically, turbulence could cause waveform distortion, drift and arrival angle fluctuation of laser beam, and eventually restrict its practical applications [4–6]. Besides that, even without turbulence, diffraction as the natural property of light could also induce laser beam divergence, in other words that waveform keep changing during propagation. [7–9].

For several decades, a variety of methods have been proposed to overcome the effect of turbulence and natural diffraction to keep laser beam propagating stably, such as nonlinear soliton [10,11], adaptive optics (AO) [12–14] and anti-diffraction beam shaping [15–19]. The soliton method resists beam broadening by using the nonlinear self-trapping effect, which needs nonlinear medium, thus not applicable for free-space propagation. AO system depends on the feedback and compensation of wavefront corrections by using complex algorithm and deformable mirror, and thus are usually associated with extraordinary high cost and complexity. Though anti-diffraction beam shaping method like Bessel [20,21] or Airy beams [22–25] have led to optical beams maintaining good shape during propagation, as have been applied in a variety of applications such as image transmission, laser communication, and detection [17,26–28], their limitations are well known and bothersome for some applications. For example, the truncation of these beams' tail by finite aperture of optical elements which is unavoidably in reality, could reduce the propagation distance of these beams severely. Actually, the longest propagation distance reported

#452190 Journal © 2022 https://doi.org/10.1364/OE.452190

<sup>&</sup>lt;sup>1</sup>Aerospace Information Research Institute, Chinese Academy of Sciences, Beijing 100094, China

<sup>&</sup>lt;sup>2</sup>School of Optoelectronics, University of Chinese Academy of Sciences, Beijing 101400, China

<sup>&</sup>lt;sup>3</sup>Science and Technology on Solid-State Laser Laboratory, Beijing 100015, China

<sup>&</sup>lt;sup>4</sup>School of Science, China University of Geosciences, Beijing 100083, China

<sup>&</sup>lt;sup>5</sup>Qilu Aerospace Information Research Institute, Jinan 250100, China

<sup>&</sup>lt;sup>6</sup>School of Eletronic Engineering, Beijing University of Posts and Telecommunications, Beijing 100876, China

<sup>&</sup>lt;sup>7</sup>The MOE Key Laboratory of Weak-Light Nonlinear Photonics, TEDA Applied Physics Institute and School of Physics, Nankai University, Tianjin 300457, China

<sup>\*</sup>zhangze@aircas.ac.cn

so far is just a few meters realized by spatial light modulators (SLMs) in laboratory environment [29–34]. To reduce the effect of turbulence and diffraction to laser beam, other kinds of methods are expected to try.

In this work, we propose and demonstrate a kind of steady optical beam (SOB) by superimposing multiple ring beams based on the mechanism of transverse wave vectors elimination. A quartz aspheric lens is employed to form a series of concentric ring beams at different distance. By interfering with each other, and eliminating transverse wave vectors, a kind of SOB that can propagate stably in turbulent environment is realized. The propagation characteristics of the SOB are studied through simulation and experiment. The measured beam parameter product (BPP) of the newly constructed SOB is approximately 50% smaller than that of Gaussian beam under the same propagation situation at certain propagation range. To verify its ability to resist turbulence effect, a comparative experiment is carried on by letting both SOB and Gaussian beam propagate through the same water turbulent environment.

### 2. Theoretical analysis

The wave function of the ring beam in the cylindrical coordinate system is expressed as

$$\mathbf{E}(\mathbf{r}, \mathbf{z}) = E_i \exp\left\{i\mathbf{k}_{\mathbf{r}} \cdot \mathbf{r} + i\mathbf{k}_z \cdot \mathbf{z}\right\},\tag{1}$$

where  $\mathbf{r}$  and  $\mathbf{z}$  denote vectors with radial and axial directions, respectively,  $E_i$  is the transverse light field amplitude distribution and it can be given as

$$E_{i} = \sqrt{I_{0}} \left\{ \exp \left[ -\frac{(\mathbf{r} - \mathbf{r}_{i})^{2}}{\omega_{i}^{2}(z)} \right] + \exp \left[ -\frac{(\mathbf{r} + \mathbf{r}_{i})^{2}}{\omega_{i}^{2}(z)} \right] \right\}, \tag{2}$$

where  $I_0$  represents initial light intensity,  $|\mathbf{r}_i|$  represents the radial distance between the position of maximum radial intensity and the center of the beam,  $\omega_i(z)$  represents beam width of the ring beam,  $\mathbf{k}_r$  and  $\mathbf{k}_z$  represent the radial wave vector and the axial wave vector, respectively. Suppose that these ring beams are arranged right next to each other at the initial plane, they will mix and interfere with each other during propagation due to diffraction broadening. At each interfere point, the combination light field of  $E_m$  and  $E_n$  can be written:

$$\mathbf{E}(\mathbf{r}, \mathbf{z}) = E_{m} \exp(i\mathbf{k}_{r} \cdot \mathbf{r} + i\mathbf{k}_{z} \cdot \mathbf{z}) + E_{n} \exp(i\mathbf{k}_{r}^{'} \cdot \mathbf{r} + i\mathbf{k}_{z} \cdot \mathbf{z}).$$
(3)

It can be easily calculated that:

$$\mathbf{E}(\mathbf{r}, \mathbf{z}) = 2\cos(\mathbf{k}_r \cdot \mathbf{r}) E_m \exp(i\mathbf{k}_z \cdot \mathbf{z}) + (E_n - E_m) \exp\left(i\mathbf{k}_r' \cdot r + i\mathbf{k}_z \cdot \mathbf{z}\right) + E_m \exp(-i\mathbf{k}_r \cdot \mathbf{r} + i\mathbf{k}_z \cdot \mathbf{z}) \left\{ \exp\left[i\left(\mathbf{k}_r' + \mathbf{k}_r\right) \cdot \mathbf{r}\right] - 1 \right\}.$$
(4)

In Eq. (4), for the situation that  $\mathbf{k}_r = -\mathbf{k}_r$  and  $E_n = E_m$ , the phase term of the radial wave vectors  $\mathbf{k}_r$  and  $\mathbf{k}_r$  is eliminated, indicating that the transverse intensity profile of the ring beam remains unchanged. The resultant light filed is:

$$\mathbf{E}(\mathbf{r}, \mathbf{z}) = 2E_m \cos(\mathbf{k}_r \cdot \mathbf{r}) \exp(i\mathbf{k}_z \cdot \mathbf{z}). \tag{5}$$

In Eq. (5), since that the phase factor doesn't have radial component, its shape could maintain during propagation, so called steady optical field.

To verify the effect of wavevector's elimination, we simulate the procedure of two ring beams' propagation, as shown in Fig. 1. In the simulation, we generate two concentric ring beams with Gaussian intensity distribution. The inner and the outer ring beams are set 0.7 mm and 2.0 mm

away from the center, respectively. Both beams have the same ring width of 0.3 mm, and the same wavelength of 532 nm. A focused phase  $\exp(-ik\beta r)$  and a defocused phase  $\exp(ik\beta r)$  are added to the outer ring beam and the inner ring beam at the initial plane, respectively, where  $\beta$  is a constant, so the two beams will mix and interfere with each other fast. It can be seen that a steady optical wave form is observed between the positions of  $z_2$  and  $z_3$ . In the range of  $z_2$  and  $z_3$ , the waveform maintains almost the same during propagation, as shown in Fig. 1(c, d).

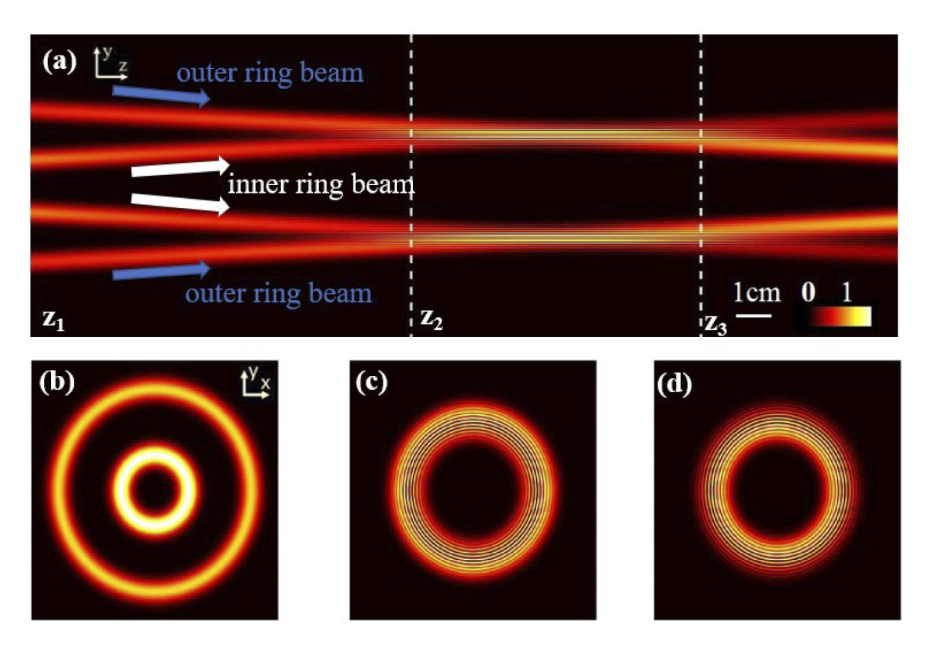


**Fig. 1.** Simulation result to illustrate the procedure of combining two ring beams. (a): The side-view. (b), (c) and (d): Transverse beam patterns at  $z_1$ =0 cm,  $z_2$ = 11.84 cm,  $z_3$ =20.88 cm.

## 3. Experimental setup and results

In experiment, we use an aspherical lens which contains multiple ring structure to split an input Gaussian beam wavefront into multiple ring wavefront and focus each ring wavefront at different position. The focal length in the center area of the aspherical lens is the smallest of all. The further the ring structure from aspherical lens center, the longer focal length it is. The specific focal length is set according to the rules: for two neighbor ring structure, the outer one focus the laser beam at the position half Rayleigh length longer than the inner one. Based on this rule, the inner beam that is supposed to diffract outward at its Rayleigh length, and meet the outer beam that is supposed to focus itself at its focal length, so they mix and interfere with each other to keep their beam form without much distortion.

The experimental setup to generate SOB and verify its propagation behavior in water turbulence is shown in Fig. 2, in which the orange box part of the figure illustrates the generation setup of SOB and the blue box part illustrates the turbulence-resistance setup. In the experiment a collimated continuous wave (CW) 532 nm laser beam with the power of 88.9 mW is expanded from 1mm to 30 mm, and split by the designed aspheric lens. The aspheric lens that is made of fused quartz contains 16 arcs with different curvature, corresponding to different focal lengths, as shown in the inset snap of Fig. 2.

A beam analyzer (Jingyi Optoelectronics) was used to collect the spot of the SOB that passed through BS2. The blue box part of Fig. 2 is the experimental setup to verify its propagation

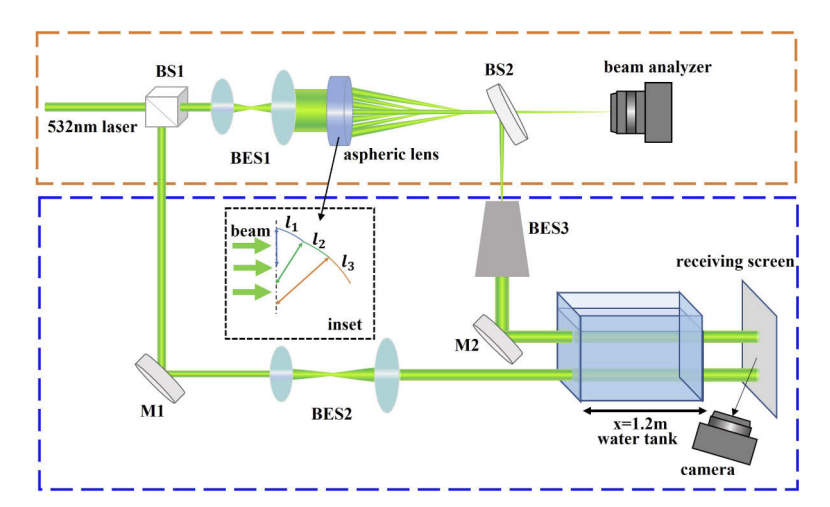
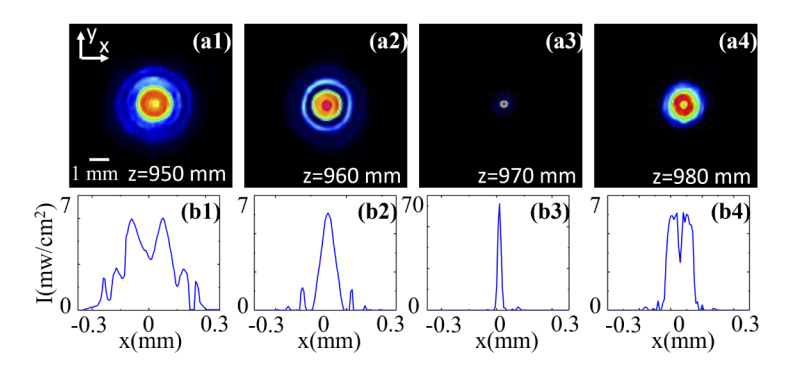


**Fig. 2.** Experimental setup to generate SOB and verify its propagation through water turbulence. The inset is a schematic diagram of the designed aspheric lens. The upper part in the orange box is the setup to generate SOB, and the lower part in the blue box is the setup to verify its propagation behavior through water turbulence. M1, M2: mirror; BS1, BS2: beam splitter; BES1,BES2,BES3: beam expanding system.

behavior through water turbulence. The Gaussian beam and the SOB are reflected respectively by the BS1 and BS2 first and then expanded and collimated by the BES2 and BES3 to reach almost the same size. During their propagation through water tank, hot water is poured in to generate turbulence. A receiving screen is placed next to the water tank to observe and record the beam spot together with a camera.

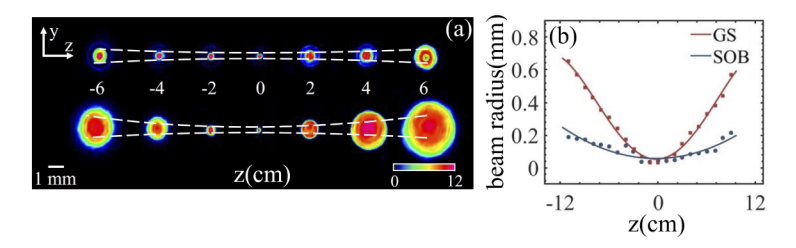
The transverse distributions of the generated SOB at different propagation distance are shown in Fig. 3(a1-a4). Taking the position of the aspheric lens as z=0 mm, the transverse intensity profiles at the distance of 950 mm, 960 mm, 970 mm and 980 mm are drawn respectively, as shown in Fig. 3(b1-b4). It can be seen that the intensity distribution of the SOB is a cosine-like form at z=950 mm where the intensity at the center is a minimal extremum. As the beam propagate further, the central light intensity increases higher and higher, while the beam radius becomes smaller and smaller, as shown in Fig. 3(a2, a3). At the position of z=950 mm, the intensity of the center of the SOB reaches to the maximum value. After that, the intensity at the center begins to decrease, as shown in Fig. 3(a4). The corresponding intensity distributions of Fig. 3(a1-a4) are shown in Fig. 3(b1-b4). It is worth to mention that the peak intensity of the beam after focusing is several times higher than other positions, which shows a self-focusing effect of such kind of beam.

To verify the anti-diffraction effect of SOB, we carried on a comparative experiment of SOB and Gaussian beam. In the experiment, we use the method of beam parameter product (BPP) to analyze the beam propagation quality. For fair comparison, the generated Gaussian beam is set to have approximately the same beam width with SOB. We set the position of the minimum beam width as the coordinate origin and captured 6 images right before and after this position, as shown in Fig. 4(a). In Fig. 4(a), we define the beam width as the length between the positions where the intensity reaches  $1/e^2$ . For the convenience of observation, the fitted curve of the beam size of both SOB and Gaussian beam is drawn, as shown of the white dashed line in Fig. 4(a). It can be seen clearly that the beam size of SOB is significantly smaller than that of the Gaussian beam at the same position, which means smaller BPP of SOB than Gaussian beam at this specific range. The detailed data of beam radii of both SOB and Gaussian beam at different distances are drawn in Fig. 4(b). It can be seen that as the distance increase, the beam



**Fig. 3.** Experimental transverse beam intensity patterns and beam profiles of the SOB at different propagation distances. (a1-a4): Beam patterns at different propagation distances. (b1-b4): Intensity profiles along x-direction at corresponding positions.

radius of the Gaussian beam increases much faster than that of the SOB. It is measured that the fitted divergence angle  $\theta$  of the SOB is 20.54 mrad while the beam waist radius  $\omega_0$  is 0.036 mm, corresponding to the BPP of 0.74 mm·mrad. The fitted divergence angle  $\theta$  of the Gaussian beam is 47.53 mrad while the beam waist radius  $\omega_0$  is 0.026 mm, corresponding to the BPP of 1.50 mm·mrad. The comparison results of the data are shown in Table 1. The BPP of the SOB is 49.40% of the Gaussian beam within a distance range of 20 mm. It proves that the SOB has much better propagation characteristics than Gaussian beam at this range.



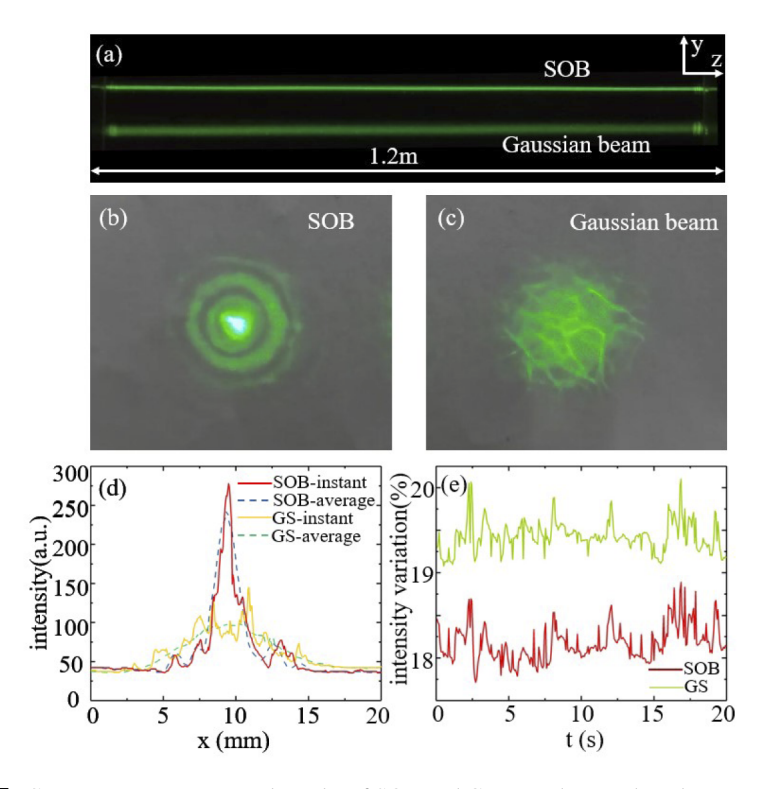
**Fig. 4.** Direct comparison of beam propagation behavior between SOB and Gaussian beam. (a): Beam patterns of SOB (upper) and Gaussian beam (lower). (b): Beam radii of SOB and Gaussian beam as a function of propagation distance.

Table 1. Beam radii of SOB and Gaussian beam at different positions.  $\omega_1$ : beam radius at 3 mm;  $\omega_2$ : beam radius at 6 mm;  $\omega_3$ : beam radius at 9 mm;  $\theta$ : fitted divergence angle; BPP: beam parameter product(the product of  $\omega_0$  and  $\theta$ ).

	$\omega_0$ /mm	$\omega_1$ /mm	$\omega_2$ /mm	$\omega_3$ /mm	$\theta$ /mrad	BPP/mm·mrad
GS	0.026	0.146	0.333	0.567	57.53	1.50
SOB	0.036	0.047	0.088	0.213	20.54	0.74

To verify the steady property of SOB, we carried on a further experiment to study the propagation behavior through water turbulence. The experiment setup is shown in the blue dotted-lined box of Fig. 2. In the experiment, we also make a comparison between Gaussian beam and SOB under the same turbulent conditions. The silica water tank we used in the experiment is 1.2m long and placed in the light propagation path. When SOB and Gaussian beam propagate through the water tank, 90°C hot water was poured into it. Meantime, we stir the water quickly to simulate the temperature gradient and fast movement of the turbulent environment. The

turbulence magnitude can be controlled well by adjusting the speed of stirring and pouring. For the convenience of observation, we added polystyrene particles in to the water, so the beam profile can be seen clearly due to scatter, as shown in Fig. 5(a). Figure 5(b) and 5(c) show the transverse beam spot of the SOB and Gaussian beam at the receiving screen. From these results, we can qualitatively conclude that the beam propagation behavior of SOB is really better than that of Gaussian beam, even they have almost the same size and propagate under the same environment. The reason of SOB to have such ability to resist turbulence effect can be easily understood. The light field depicted in Eq. (5) is a stable wave field, which means that each interference process generates this same wave field. In other words, the same wave field kept being generated at different position to maintain this same beam spot during propagation.



**Fig. 5.** Comparative experimental results of SOB and Gaussian beam when they propagate in stationary water (a) and turbulent water (b, c). (a): Side-view of beam profiles of SOB and Gaussian beam passing through water tank without turbulence. (b, c): Beam spot of the SOB (b) and the Gaussian beam (c) after passing through turbulent water(see Visualization 1 for the complete video). (d): Comparison of intensity distribution of SOB and Gaussian beam, in which time-averaged mean intensity profile of the SOB is marked with blue dashed line, and that of the Gaussian beam is marked with green dashed line; the instantaneous intensity of the SOB is marked with red solid curve, and that of Gaussian beam is marked with orange solid line. (e): Percentage of relative intensity fluctuation as a function of time of the SOB (red line) and Gaussian beam (orange line), as defined by Eq. (6).

To quantificationally compare the propagation behavior, we recorded 300 frames of the beam spots of both SOB and Gaussian beam when they propagate the same turbulent environment during a time interval about 20 s. With these beam spots, we use Eq. (6) to calculate both time

and space intensity fluctuation of SOB and Gaussian beam.

$$\Delta I_t = \frac{\int \int |I(x, y, t) - I_{mean}(x, y)| dxdy}{\int \int I_{mean}(x, y) dxdy},$$
(6)

where I(x, y, t) is the instantaneous intensity at a certain moment,  $I_{mean}(x, y)$  is the time-averaged intensity. The calculated I(x, y, t) and  $I_{mean}(x, y)$  of both SOB Gaussian beams are shown with the blue dashed line, red solid line, orange solid line, green dashed line respectively in Fig. 5(d). It can be seen that the I(x, y, t) and  $I_{mean}(x, y)$  of Gaussian beam are very different, while the ones of SOB are almost the same. This evidently indicates that SOB is more stable than Gaussian beam. For further calculations, we substitute the intensity distribution of SOB and Gaussian into Eq. (6) to analyze the intensity fluctuation of these two beams according to time. The calculated results are shown in Fig. 5(e). The results also show that SOB has better performance than Gaussian beam in turbulent environment.

#### 4. Conclusion

In summary, we have theoretically proposed and experimentally demonstrated a method to generate the SOB by superposition of ring beams with different focal length. The propagation property of the SOB is verified in both free space and turbulent environment by making comparison with Gaussian beam. It is found that this SOB has weak divergence at certain range, and good ability to resist turbulence effect. The method to construct SOB is believed to have great prospects for applications that require laser beam to propagate into long distance, especially in turbulent environment, such as laser communication, laser detection, and remote sensing.

**Funding.** National Natural Science Foundation of China (No.12074350, No.62105341); Natural Science Foundation of Shandong Province (No.ZR2021QF126); Science and Technology on Solid-State Laser Laboratory stability support project.

**Disclosures.** The authors declare no conflicts of interest.

**Data availability.** Data underlying the results presented in this paper are not publicly available at this time but may be obtained from the authors upon reasonable request.

#### References

- J. C. Ricklin and F. M. Davidson, "Atmospheric turbulence effects on a partially coherent gaussian beam: implications for free-space laser communication," J. Opt. Soc. Am. A 19(9), 1794

  –1802 (2002).
- 2. H. T. Yura, "Atmospheric turbulence induced laser beam spread," Appl. Opt. 10(12), 2771–2773 (1971).
- 3. V. A. Kulikov and M. A. Vorontsov, "Analysis of the joint impact of atmospheric turbulence and refractivity on laser beam propagation," Opt. Express 25(23), 28524–28535 (2017).
- 4. L. Zhang, Z. Xu, T. Pu, H. Zhang, J. Wang, and Y. Shen, "Change in the state of polarization of gaussian schell-model beam propagating through non-kolmogorov turbulence," Results Phys. 7, 4332–4336 (2017).
- L. Cui, "Effects of anisotropic turbulence on the long term beam spread and beam wander of gaussian beam," Optik 163, 152–158 (2018).
- J. T. Coffaro, B. Berry, M. Salfer-Hobbs, R. L. Philips, L. C. Andrews, R. F. Crabbs, and C. Smith, "Exploring the behavior of supercontinuum laser sources in atmospheric turbulence," in *Laser Communication and Propagation* through the Atmosphere and Oceans IX, vol. 11506 J. A. Anguita, J. P. Bos, and D. T. Wayne, eds., International Society for Optics and Photonics (SPIE, 2020), pp. 76–88.
- Y. Wang, Q. Chen, H. Li, G. Ren, R. Zhu, and X. Zhou, "The simulation of laser diffraction effect in optoelectric imaging systems," in *Fourth Seminar on Novel Optoelectronic Detection Technology and Application*, vol. 10697 W. Jin and Y. Li, eds., International Society for Optics and Photonics (SPIE, 2018), pp. 68–78.
- M. Golshani and M. Motamedifar, "Impact of aperture thickness on a fraunhofer diffraction pattern," J. Opt. 21(4), 045605 (2019).
- Z. Liu, T. Pu, J. Niu, L. Shi, and C. Xie, "High-efficiency v-shaped phase gratings to suppress high order diffractions," AIP Adv. 9(1), 015308 (2019).
- 10. Y. S. Kivshar and G. Agrawal, Optical solitons: from fibers to photonic crystals (Academic press, 2003).
- Z. Chen, M. Segev, and D. N. Christodoulides, "Optical spatial solitons: historical overview and recent advances," Rep. Prog. Phys. 75(8), 086401 (2012).
- 12. R. Davies and M. Kasper, "Adaptive optics for astronomy," Annu. Rev. Astron. Astrophys. 50(1), 305-351 (2012).

- 13. M. J. Booth, "Adaptive optical microscopy: the ongoing quest for a perfect image," Light: Sci. Appl. 3(4), e165 (2014).
- J. C. Christou, J. Girkin, C. Kulcsár, and L. K. Young, "Feature issue introduction: applications of adaptive optics," Opt. Express 29(8), 11533–11537 (2021).
- 15. D. McGloin and K. Dholakia, "Bessel beams: Diffraction in a new light," Contemp. Phys. 46(1), 15-28 (2005).
- C. Vetter, R. Steinkopf, K. Bergner, M. Ornigotti, S. Nolte, H. Gross, and A. Szameit, "Realization of free-space long-distance self-healing bessel beams," Laser Photonics Rev. 13(10), 1900103 (2019).
- N. K. Efremidis, Z. Chen, M. Segev, and D. N. Christodoulides, "Airy beams and accelerating waves: an overview of recent advances," Optica 6(5), 686–701 (2019).
- 18. X. Weng, Q. Song, X. Li, X. Gao, H. Guo, J. Qu, and S. Zhuang, "Free-space creation of ultralong anti-diffracting beam with multiple energy oscillations adjusted using optical pen," Nat. Commun. 9(1), 5035 (2018).
- Z. Zhang, X. Liang, M. Goutsoulas, D. Li, X. Yang, S. Yin, J. Xu, D. N. Christodoulides, N. K. Efremidis, and Z. Chen, "Robust propagation of pin-like optical beam through atmospheric turbulence," APL Photonics 4(7), 076103 (2019).
- 20. J. Durnin, "Exact solutions for nondiffracting beams. i. the scalar theory," J. Opt. Soc. Am. A 4(4), 651-654 (1987).
- 21. J. Durnin, J. J. Miceli, and J. H. Eberly, "Diffraction-free beams," Phys. Rev. Lett. 58(15), 1499–1501 (1987).
- G. A. Siviloglou, J. Broky, A. Dogariu, and D. N. Christodoulides, "Observation of accelerating airy beams," Phys. Rev. Lett. 99(21), 213901 (2007).
- G. A. Siviloglou and D. N. Christodoulides, "Accelerating finite energy airy beams," Opt. Lett. 32(8), 979–981 (2007).
- P. Zhang, J. Prakash, Z. Zhang, M. S. Mills, N. K. Efremidis, D. N. Christodoulides, and Z. Chen, "Trapping and guiding microparticles with morphing autofocusing airy beams," Opt. Lett. 36(15), 2883–2885 (2011).
- 25. Z. Zhang, P. Zhang, M. Mills, Z. Chen, D. N. Christodoulides, and J. Liu, "Trapping aerosols with optical bottle arrays generated through a superposition of multipleairy beams," Chin. Opt. Lett. 11(3), 033502 (2013).
- Y. Liang, Y. Hu, D. Song, C. Lou, X. Zhang, Z. Chen, and J. Xu, "Image signal transmission with airy beams," Opt. Lett. 40(23), 5686–5689 (2015).
- 27. Y. Yuan, T. Lei, Z. Li, Y. Li, S. Gao, Z. Xie, and X. Yuan, "Beam wander relieved orbital angular momentum communication in turbulent atmosphere using bessel beams," Sci. Rep. 7(1), 42276 (2017).
- 28. S. H. Moosavi, C. Gohn-Kreuz, and A. Rohrbach, "Feedback phase correction of bessel beams in confocal line light-sheet microscopy: a simulation study," Appl. Opt. **52**(23), 5835–5842 (2013).
- M. Duocastella and C. Arnold, "Bessel and annular beams for materials processing," Laser Photonics Rev. 6(5), 607–621 (2012).
- S. Akturk, B. Zhou, M. Franco, A. Couairon, and A. Mysyrowicz, "Generation of long plasma channels in air by focusing ultrashort laser pulses with an axicon," Opt. Commun. 282(1), 129–134 (2009).
- H. E. Kondakci and A. F. Abouraddy, "Airy wave packets accelerating in space-time," Phys. Rev. Lett. 120(16), 163901 (2018).
- B. Bhaduri, M. Yessenov, and A. F. Abouraddy, "Meters-long propagation of diffraction-free space-time light-sheets," Opt. Express 26(16), 20111–20121 (2018).
- 33. W. Nelson, J. P. Palastro, C. C. Davis, and P. Sprangle, "Propagation of bessel and airy beams through atmospheric turbulence," J. Opt. Soc. Am. A 31(3), 603–609 (2014).
- 34. N. Mphuthi, R. Botha, and A. Forbes, "Are bessel beams resilient to aberrations and turbulence?" J. Opt. Soc. Am. A 35(6), 1021–1027 (2018).